J. Phys. Chem. A 2006, 110, 10155−10162

Theoretical Determination of the Rate Constant for OH Hydrogen Abstraction from Toluene

Víctor H. Uc,[†] J. Raúl Alvarez-Idaboy,*[,‡] Annia Galano,[†] Isidoro García-Cruz,[†] and Annik Vivier-Bunge[§]

Instituto Mexicano del Petróleo, Eje Central Lázaro Cardenas 152, México D.F. 07730, México, Facultad de Química, Universidad Nacional Autónoma de México, Ciudad Universitaria, México D.F. 04510, México, and Área de Química Cuántica, Departamento de Química, Universidad Autónoma Metropolitana, Unidad Iztapalapa, México City C.P. 09340, México

Received: May 6, 2006; In Final Form: July 4, 2006

The OH abstraction of a hydrogen atom from both the side chain and the ring of toluene has been studied in the range 275−1000 K using quantum chemistry methods. It is found that the best method of calculation is to perform geometry optimization and frequency calculations at the BHandHLYP/6-311++G(d,p) level, followed by CCSD(T) calculations of the optimized structures with the same basis set. Four different reaction paths are considered, corresponding to the side chain and three possible ring hydrogen abstractions, and the branching ratio is determined as a function of temperature. Although negligible at low temperatures, at 1000 K ring-H abstraction is found to contribute 11% to the total abstraction reaction. The calculated rate coefficients agree very well with experimental results. Side chain abstraction is shown to occur through a complex mechanism that includes the reversible formation of a collisionally stabilized reactant complex.

1. Introduction

It is well-known that the reaction of toluene with OH radicals[1,2] occurs according to three possible pathways: abstraction of a hydrogen atom from either the side chain

$$C_6H_5CH_3 + OH^\bullet \rightarrow C_6H_5CH_2^\bullet + H_2O \quad (1)$$

or the ring

$$C_6H_5CH_3 + OH^\bullet \rightarrow C_6H_4CH_3^\bullet + H_2O \quad (2)$$

and addition of the OH radical to the ring

$$C_6H_5CH_3 + OH^\bullet \rightarrow C_6H_5(OH)CH_3^\bullet \quad (3)$$

Reactions 1 and 2 are especially important at high temperatures such as those occurring in fuel combustion processes, and reaction 3 is dominant in tropospheric conditions.

The kinetics and mechanism of the OH radical reaction with toluene have been reviewed and evaluated by Atkinson.[3,4] The rate of OH decay for toluene was first recorded by Perry et al.[5] over the temperature range 296−473 K at a total pressure of about 100 Torr of argon. As the temperature is increased from about 298 K, a complex behavior is observed.[1] At room temperature, the OH radical decay is exponential, with the rate constant decreasing slightly as temperature increases, thus presenting a positive slope in an Arrhenius plot of log k against $1/T$. For temperatures between 325 and 380 K, the OH decay is no longer exponential and an abrupt change is observed both in the value and in the sign of the slope. For temperatures above 380 K, the OH decay is again exponential, with a negative slope of the Arrhenius plot.

The highly curved Arrhenius plots have been explained by the competition between different possible pathways, whose relative importance varies with temperature. At room temperature and atmospheric pressure, the H-atom abstraction pathways have been estimated to occur in about 10% of the events. Finlayson[1] has pointed out that, when abstractable hydrogen atoms are available on an alkyl side chain, abstraction occurs from the substituent alkyl groups, because these C−H bonds are much weaker (=85 kcal/mol) than those involving carbon atoms from the ring (=110 kcal/mol). However, from a comparison of rate constant measurements for H-abstraction from benzene and toluene, Tully et al. estimated[2] that, at 500 K, the contribution of the ring hydrogen abstraction channel to the overall rate constant could be about 20%. Thus, at high temperatures, ring hydrogen abstraction is probably not negligible.

Side chain abstraction leads to the formation of a benzyl radical which, in the presence of molecular oxygen, yields benzaldehyde. Several authors[2,6,7] have proposed rate expressions for the OH side chain hydrogen abstraction in toluene. Most values reported in the NIST database[8] for the activation energy fall between 0.5 and 0.9 kcal/mol,[5−7] although these values do not correspond to Arrhenius-type rate expressions. An exception is the result of $E_a = 2.583$ kcal/mol estimated by Tully et al.[2] from measurements between 500 and 1000 K using isotopic substitution reactions in benzene and toluene OH hydrogen abstractions. An expression for the rate constant over the 400−1200 K temperature range has been given by Baulch et al.:[7] $k = 8.6 \times 10^{-15}T \exp(-440/T)$ molecule^{-1} s^{-1}. The abstraction rate constant at room temperature has also been obtained by Markert and Pagsberg[9] who report a value of $(7 \pm 1) \times 10^{-13}$ molecule^{-1} s^{-1} at 338 K, in good agreement with

---

[†] Instituto Mexicano del Petróleo.
[‡] Universidad Nacional Autónoma de México.
[§] Universidad Autónoma Metropolitana.

10.1021/jp062775l CCC: $33.50

the result obtained by Knispel et al. (4.25×10^{-13} molecule^{-1} s^{-1}) at 298 K.

Although the addition reaction of OH to toluene has been studied theoretically by several authors,[10−13] no theoretical work is available for the OH hydrogen abstraction from either the methyl side chain or the ring of toluene. In previous work[11] we have identified a stable pre-reactive [OH···toluene] complex that plays a significant role in the addition mechanism. The structure and type of long range attractions that are responsible for the stability of this complex were thoroughly dicussed in ref 11. Its existence is essential to explain the negative activation energy observed at low temperatures. If it were found to also play a role in the H-abstraction processes, it would be essential for the correct calculation of the tunnel effect. More recently, Tokmakov and Lin[14] have performed energy and kinetics calculations for addition and abstraction in the benzene + OH reaction. For the addition channel they identified a pre-reactive complex, which is very similar to the one previously reported by us for toluene.[11]

In the present work, we shall study the abstraction process in toluene + OH for both the methyl and the ring hydrogen atoms. For abstraction of the methyl hydrogens, a mechanism that involves a pre-reactive complex will be investigated. Rate coefficients in the range 275−1000 K will be determined for the side chain and the ring hydrogen abstractions, as well as for the overall reaction. Reaction 1 is the natural extension of our work on hydrogen abstraction reactions in alkanes.[15−17] The relative weight of ring vs side chain abstraction at different temperatures will be estimated.

2. Computational Methodology

The side chain hydrogen abstraction is studied first. Electronic structure calculations are performed mainly with the system of programs Gaussian98 (G98).[18] Restricted and unrestricted Hartree−Fock theory is used for closed and open shell systems, respectively. The convenience of using several methods of calculation simultaneously has often been stressed, especially in the case of radical−molecule reactions, because different methods seem to be more reliable for different types of systems. Thus, on the basis of our previous experience on toluene reactions with several radicals,[11,19,20] all geometries for the methyl hydrogen abstraction reaction are fully optimized both with Møller−Plesset perturbation theory up to second order (MP2(FC)) and with density functional theory (DFT), using mainly the BHandHLYP hybrid functional[21] and the 6-31G(d,p) and 6-311++G(d,p) basis sets. In addition, single point BHandHLYP energy calculations are obtained with larger basis sets (AUG-cc-pVTZ, 6-311++G(d,p)). Also, the CCSD(T) method has been used with the 6-311++G(d,p) basis set at the BHandHLYP geometry.

In the perturbation theory calculations, projected MP2 energies (PMP2) are used throughout to correct for spin contamination.

Frecuency calculations are carried out for all stationary points at the DFT and MP2(FC)levels of theory. Local minima and transition states are identified by the number of imaginary frequencies (NIMAG=0 or 1, respectively). An intrinsic reaction coordinate calculation (IRC)[22] is performed at the BHandHLYP/6-311++G(d,p) level on both sides of the transition state to ensure that it connects reactants and products as expected.

Zero point energies (ZPE) at 298.15 K are included in the determination of energy barriers and heats of reaction, respectively.

In the side chain abstraction, a pre-reactive complex is involved, and a complex mechanism will be assumed to occur.[23] It is a two-step mechanism that involves a fast preequilibrium between the reactants and the pre-reactive complex:

$$\text{Step 1:} \qquad C_6H_5CH_3 + OH^{\bullet} \leftrightarrow [C_6H_5CH_3\cdots OH]^{\bullet} \tag{4}$$

followed by a transition state leading to products. The second step is an internal rearrangement leading to the elimination of a water molecule:

$$\text{Step 2:} \qquad [C_6H_5CH_3\cdots OH]^{\bullet} \rightarrow C_6H_5CH_2^{\bullet} + H_2O \tag{5}$$

If k_1 and k_{-1} are the rate constants for the forward and reverse reactions in the first step and k_2 corresponds to the second step, a steady-state analysis leads to a rate constant for the overall reaction which can be written as

$$k = \frac{k_1 k_2}{k_{-1}} = \left(\frac{A_1 A_2}{A_{-1}}\right) \exp[-(E_1 + E_2 - E_{-1})/RT] \tag{6}$$

Because E_1 is zero, the net activation energy for the overall reaction is

$$E_a = E_2 - E_1 = (E_{TS} - E_{P-R}) - (E_R - E_{P-R}) = E_{TS} - E_R \tag{7}$$

where E_R, E_{P-R} and E_{TS} are the total energies of the reactants, the pre-reactive complex, and the transition state, respectively. Thus, the activation energy at high pressures can be calculated as the difference between the energy of the transition state and that of the reactants, without having to obtain the energy of the pre-reactive complex.

Applying basic statistical thermodynamic principles, the equilibrium constant of the fast equilibrium between the reactants and the pre-reactive complex may be obtained as

$$K_{eq} = \frac{Q_{P-R}}{Q_R} \exp[E_R - E_{P-R}/RT] \tag{8}$$

where Q_{P-R} and Q_R are the pre-reactive complex and the reactants partition functions, respectively. Under high-pressure conditions, an equilibrium distribution of reactants is established, and the classical TST formula can be used[24] to calculate k_2:

$$k_2 = \sigma\kappa \frac{k_B T}{h} \frac{Q_{TS}}{Q_{P-R}} \exp[E_{P-R} - E_{TS}/RT] \tag{9}$$

where κ is the tunneling factor. As in previous works for similar mechanisms, we have assumed that in the channel that occurs via the prereactant complex it undergoes collisional stabilization; i.e., this reaction step occurs in a high-pressure limit. Sigma is the reaction path degeneracy that accounts for the number of equivalent reaction paths. The partition functions are obtained from the rotational constants and the vibrational frequencies of the ab initio and DFT calculations.

Finally, the rate constant can be written as

$$k = K_{eq} k_2 \tag{10}$$

or

$$k = \sigma\kappa \frac{k_B T}{h} \frac{Q_{TS}}{Q_R} \exp[E_R - E_{TS}/RT] \tag{11}$$

It is important to note that this expression does not involve the pre-reactive complex explicitly. However, the latter is present in the value of the tunneling factor κ, which depends on the height and shape of the activation barrier of the elementary process in which the hydrogen atom is abstracted. If the pre-reactive complex is not taken into account, the barrier is smaller, and the corresponding tunneling factor is also smaller. Thus, neglect of the pre-reactive complex leads to an incorrect tunneling coefficient.

Rate coefficients are calculated using transition state theory (TST) as implemented in TheRate program 1.0.[25] The calculated reaction rate constant for abstraction of a hydrogen atom from the side chain of toluene must be multiplied by a factor of 3, to take into account the three hydrogen atoms in the methyl group. The ring rate constant is obtained from individual rate constants for hydrogen abstraction from the ortho, meta and para positions. The tunneling correction is defined as the ratio of the quantum-mechanical to the classical barrier crossing rate, and it is calculated here assuming an unsymmetrical, one-dimensional, Eckart function barrier.[26]

The results of the thermochemical calculation included in the Gaussian98 vibrational output are used with corrections as described next. In the Gaussian98 standard version, the energy levels of all vibrations, and their corresponding partition function contribution, are calculated using the harmonic oscillator approximation. However, some of these vibrations are in fact hindered internal rotations.[27] This implies that, for systems with internal rotations, the partition functions may be underestimated. In general, it is accepted that, for internal rotations with barriers smaller than about 3.0 kcal/mol, vibrational partition functions should be replaced by the ones corresponding to hindered internal rotations. For example, in the ring abstraction reaction transition state of toluene, there are two internal rotations to be considered, corresponding to rotation of OH and of the methyl group. A calculation must be performed to determine their corresponding rotation barrier. If it is smaller than 3.0 kcal/mol, the contribution to the partition function should be calculated using the expression for the hindered rotor (Q_{hind}). In our calculations we have adopted the analytical approximation to Q_{hind} for a one-dimensional hindered internal rotation proposed by Ayala and Schlegel.[28]

A comparison between the methyl hydrogen abstraction calculated rate constant and available experimental values at room temperature suggests that, in this problem, the method of choice to calculate the quantum chemistry energies is the CCSD(T) method with the 6-311++G(d,p) basis set at the BHandHLYP/6-311++G(d,p) geometry (abbreviated as CCSD(T)//BHandHLYP). Thus, only this method is used to determine the energy profiles for the ring hydrogen abstractions.

3. Results and Discussion

3.1. Energetics. As reactants approach each other, a decrease in energy is observed first, and a shallow minimum, corresponding to the pre-reactive complex is located, whose energy is 4.37 and 2.57 kcal/mol below reactants at the PMP2/6-311++G(d,p) and BHandHLYP/6-311++G(d,p) levels, respectively. The existence of such minima has been observed theoretically in many cases.[11,29−33] It has been shown[11,33] that pre-reactive complexes are fundamental in that they guide the reaction from the beginning and also have a strong effect on the reaction barrier height. They are weakly bound complexes that result from van der Waals interactions, and they occur when the reactants are still quite separated. Smith and Ravishankara[34] have described these systems, which are generally too short-lived to be detected, and whose existence can only be inferred by the way they affect the overall behavior of the reaction.

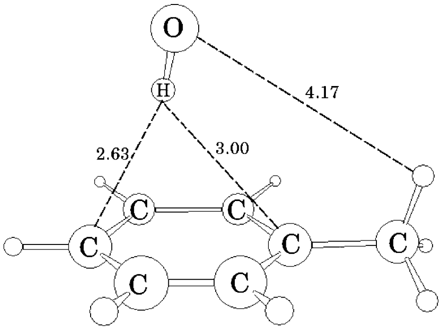

Figure 1. BHandHLYP/6-311++G** optimized pre-reactive complex. Interatomic distances are given in Å.

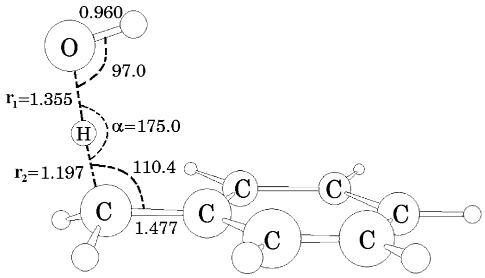

Figure 2. BHandHLYP/6-311++G** optimized transition state for the side chain hydrogen abstraction (TS_s). Interatomic distances are given in Å.

TABLE 1: Comparison of Main Geometrical Parameters (Bonds, Å; Angles, deg) of TS_s with Corresponding Values in Primary Hydrogen Atom Abstraction in Small Alkanes[a]

	O···H (r_1)	O−H (bond)	C···H (r_2)	O···H···C (α)
CH_4···OH	1.29/1.23	0.96/0.96	1.20/1.25	168.59/171.18
C_2H_6···OH	1.34/1.27	0.97/0.95	1.18/1.22	165.57/170.66
C_3H_8···OH_{prim}	1.34/1.27	0.97/0.95	1.18/1.23	164.50/170.15
toluene···OH	1.32/1.35	0.97/0.96	1.19/1.20	163.7/175.0

[a] The results correspond to MP2/6-311++G** and BHandHLYP/6-311++G** optimizations (indicated as MP2/BHandHLYP).

The geometry of the pre-reactive complex, optimized with the BHandHLYP method, is shown in Figure 1. This structure is the same as the one we identified in the case of the OH addition reaction to toluene.[11] A thorough search of the potential energy surface did not yield any other van der Waals complex with an energy lower than reactants. The pre-reactive complex has C_s symmetry, the OH radical is seen to be approaching the aromatic ring from above, H first, and at a distance of 2.3−2.4 Å from the plane of the aromatic ring. The OH radical is not fully perpendicular to the ring, being a little bent toward the methyl group, due to a weak interaction between the oxygen and the perpendicular hydrogen of CH_3. A frequency calculation yields only positive frequencies, thus ensuring that the structure is a true minimum. A low vibration at about 30 cm^{-1} clearly corresponds to an approaching motion between the oxygen atom and a methyl hydrogen, thus favoring abstraction.

In ref 11 we discussed the fact that the structure of the pre-reactive complex differs significantly from the one in alkene−OH pre-reactive complexes, in which the H of the OH radical points toward the center of the π orbital, i.e., toward the maximum electron density at the center of the C═C bond. By analogy, when an aromatic system is involved in a π complex, one would expect that the H atom of the OH radical would point toward any of the C−C bonds. In the aromatic−OH complex instead, the OH hydrogen atom is directed toward the

TABLE 2: Energies (in kcal/mol) in the Toluene + OH Side Chain Hydrogen Abstraction Reaction, Relative to the Separated Reactants, Calculated with Various Methods, at the BHandHLYP/6-311++G Optimized Geometry**

	BH&HLYP 6-311++G**	BH&HLYP 6-311++G(3df,2p)	BH&HLYP AUG-cc-pVTZ	PMP2 6-311++G**	CCSD(T) 6-311++G**
prereactive complex	−2.57	−2.47	−2.08	−4.37	−4.20
TS_s	3.26	3.28	3.42	3.30	2.54
benzyl + H_2O	−24.28	−25.19	−25.12	−28.72	−23.56

center of the phenyl ring, a point that corresponds to a minimum in the electron density distribution. In ref 11, we have used Bader's analysis[35,36] to discuss this point.

3.1.1. Side Chain Hydrogen Abstraction. In the side chain hydrogen abstraction reaction (eq 1), the reaction coordinate is, essentially, the C···H distance between the H atom that is being abstracted and the C atom of the methyl group.

The optimized geometry of the side chain transition state (TS_s) calculated at the BHandHLYP/6-311++G(d,p) level is represented in Figure 2, where we have indicated the main angles and distances. This structure was very difficult to obtain. In the first attempt, MP2 was used with the 6-31G(d,p) basis set. A transition state was obtained that presented a barrier of about 10 kcal/mol with respect to the isolated reactants, a value that is much too large in comparison with most experimental results (E_a experimental is smaller than 0.9 kcal/mol).[8] In this structure, the OH radical lies in the plane of the ring and points toward a hydrogen atom that also lies in the plane. By fixing the OH group over the benzene plane and parallel to the ring, which is a reasonable assumption, we obtained a transition state-like structure, whose energy lies 7.3 kcal/mol above reactants. If all constraints were lifted, however, it was not possible to obtain a transition state with this method and the same basis set. Including diffuse functions eventually produced a structure with an even larger barrier (10.6 kcal/mol). Finally, starting from the latter geometry and using the BHandHLYP method with the 6-311++G(d,p) basis set, a transition state was obtained that presented an activation energy of 3.26 kcal/mol. This value is still too large, but one can expect that tunneling may play an important role and help lower the effective barrier. An IRC[22] calculation performed on both sides of this transition state using the BHandHLYP method and the 6-311++G(d,p) basis set clearly leads to the pre-reactive complex on one side and to the expected products on the other side.

The main geometrical parameters of TS_s as obtained with both methods are compared in Table 1. The complete set of Cartesian coordinates is given in Supporting Information.

As already observed in ref 17 in the case of alkanes, the C···H abstraction distance is slightly larger in the BHandHLYP structure than in the MP2 structure, whereas the H···O forming bond distance is correspondingly smaller in the former method. The side chain transition state turns out to be similar to the ones previously obtained for OH abstraction of a primary hydrogen atom from alkanes.[15] In Table 1, geometrical parameters for the abstraction transition state in methane, ethane and for the primary hydrogen atoms in propane are also reported for comparison. Thus, (TS_s) is characterized by the following general properties:

1. It is closer from reactants than from products: C···H distances are smaller than H···O's, meaning that it occurs at the beginning of the reaction, when the OH$^\bullet$ radical is still somewhat far apart. This result is in agreement with the Hammond postulate, according to which transition states of exothermic reactions should be more reactant-like than product-like. However, whereas for alkanes, the H···O distance is typically about 1.29 Å, in toluene it is 1.33 Å, indicating that in the latter the OH radical is further from the hydrogen atom that is being abstracted. In fact, in toluene, TS_s is a very early transition state, the C···H distance being less than 0.1 Å from the normal C−H bond in the methyl group of toluene.

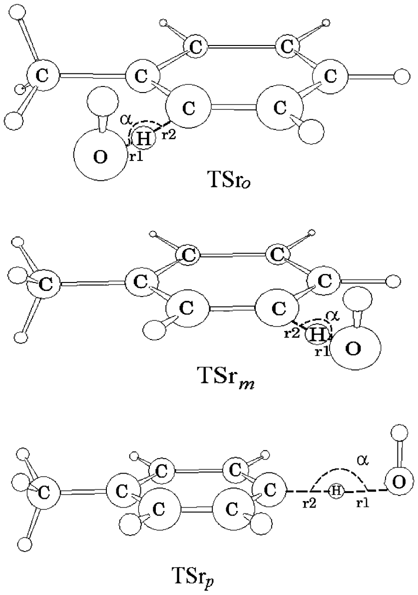

Figure 3. BHandHLYP/6-311++G** optimized transition state geometries for abstraction of an ortho (TSr_o), meta (TSr_m) and para (TSr_p) hydrogen atom from the benzene ring in toluene.

TABLE 3: BHandHLYP/6-311++G Main Geometrical Parameters (Bonds, Å; Angles, deg) in the Ring Hydrogen Abstraction Transition State (r_1 = O···H, r_2 = C···H, See Figure 3)**

	r_1	r_2	α
ortho	1.208	1.264	169.7
meta	1.204	1.265	168.8
para	1.200	1.268	168.7

2. The C···O distance in C···H···O is approximately equal to 2.5 Å.

3. The C···H···O angle is close to 164° (as compared with 170° for primary alkanes). It is curved in a direction that is such that the H of the OH$^\bullet$ radical is in a cis position to the C atom, and pointing toward the center of the ring.

The transition vector for side chain H abstraction clearly shows the approach of the OH radical toward a hydrogen atom of the methyl group.

The products, a benzyl radical and water, were readily obtained. The benzyl radical is a perfectly planar symmetric structure with the spin density clearly localized on the dehydrogenated carbon atom.

The total PMP2/6-311++G(d,p) and BHandHLYP/6-311++G-(d,p) optimized energies and the ZPE of reactants, the pre-reactive complex, the transition state and the products in the OH radical + toluene side chain abstraction reaction are available as Supporting Information. At the transition states, $\langle S^2 \rangle$ values are about 1.096 before projection, and these values are reduced to about 0.85 after projection of quartet spin states. Thus, states with multiplicity higher than 4, which are not projected in PMP2 energies, still contribute a little. The

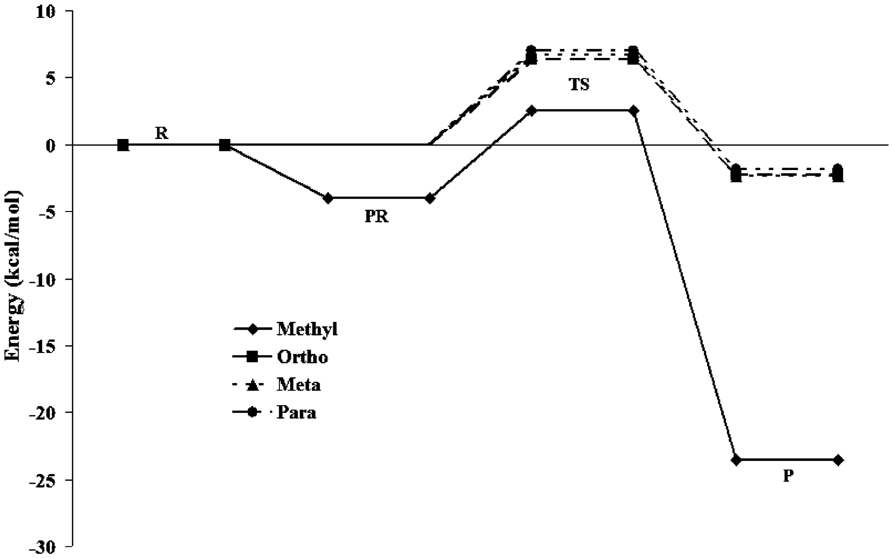

Figure 4. CCSD(T)/6-311++G**//BHandHLYP/6-311++G** energy profile for the ring and methyl hydrogen abstractions.

corresponding $\langle S^2\rangle$ values for the density functional calculations are, in general, about 0.77 before projection and very close to 0.75 after projection. The imaginary frequency (ν_i) characterizing the transition state, obtained at both levels of optimization, is 2020 and 1351 cm^{-1}, at the MP2 and BHanHLYP levels, respectively. Although very different, both values are rather large and indicate a tight transition state with a large curvature, thus favoring tunneling. In the case of alkanes, Bravo et al.[17] have obtained very good agreement between experimental and theoretical rate constants for the overall alkane + OH reaction, using geometries and partition functions calculated with the BHandHLYP method. Thus, in this work, several methods and basis sets were used to recalculate the energy values of all stationary points at their BHandHLYP optimized geometry, in an effort to obtain an activation energy that is closer to the experimentally determined values. The corresponding numerical values of the relative energies are reported in Table 2, in kcal/mol, with respect to the separated reactants, including the zero point energy correction calculated using the BHandHLYP frequencies. At the CCSD(T) level, the pre-reactive complex is seen to be stable by more than 4 kcal/mol, whereas the transition state is 2.54 kcal/mol above reactants. All the methods yield transition barriers that are consistently about 3 kcal/mol, and the CCSD(T) result is the lowest one. It is still considerably larger than the experimental result (0.5−0.9 kcal/mol), but tunneling is expected to lower the effective barrier, as observed by Bravo et al.[17] for the rate constants of several small alkanes. For example, the relative energy of the OH abstraction transition state in methane, at the CCSD(T)//BHandHLYP level and including ZPE corrections, is 7.78 kcal/mol, the tunneling factor is 30.56 and the E_a kinetic parameter obtained from the calculated kinetic data at different temperatures is 3.53 kcal/mol.[17] This value is very close to the experimental value, which is 3.50 kcal/mol. Analogously, the reaction path barrier in ethane is 4.71 kcal/mol, κ is 6.92 and E_a is 2.77 kcal/mol (the experimental value is 2.05).

The CCSD(T) reaction energy, which in this case is equal to ΔH, is about −24 kcal/mol. The best agreement with the experimental value obtained from the heats of formation of reactants and products[8] ($\Delta H = -29.56$ kcal/mol) is obtained with the PMP2/6-311++G(d,p) method.

3.1.2. Ring Hydrogen Abstraction. The BHandHLYP method was employed to optimize the transition state geometries for abstraction of an ortho, meta and para hydrogen atom from the benzene ring. Structures are labeled TSr$_o$, TSr$_m$, TSr$_p$, and they are shown in Figure 3. The most relevant parameters are given in Table 3. In all of them, the oxygen atom of the OH radical lies in the plane of the ring, whereas the O−H bond is almost perpendicular to this plane. It can be seen that the O···H and C···H distances are more symmetrical than in TS$_s$, these distances being about 1.20 and 1.26 Å, respectively. In fact, in these structures, the hydrogen atom has almost been transferred to oxygen to form a water molecule. Thus, these transition states occur much later than in the case of the side chain hydrogen abstraction, and they have considerably larger barriers, as expected from the very small exothermicity of the reaction (about −2 kcal/mol at the CCSD(T) level). That the ring channels do not involve the pre-reactive complex in Figure 1 has been verified by performing IRC calculations[22] from the corresponding transition states. No other pre-reactive complex or transition state has been identified. This is in agreement with the results obtained by Tokmakov and Lin[14] for the OH hydrogen abstraction in benzene.

BHandHLYP/6-311++G(d,p) energies of reactants, the transition states and the products in the OH radical + toluene side chain abstraction reaction are reported as Supporting Information. Spin contamination is negligible in all cases. Relative

TABLE 4: BHandHLYP/6-311++g and CCSD(T)/6-311++G**//BHandHLYP/6-311++g** Relative Energies (in kcal/mol) of the Transition States and Products, Including ZPE Corrections, for the Ring Hydrogen Abstraction Reactions**

	BHandHLYP		CCSD(T)	
	TS$_r$	products	TS$_r$	products
ortho	9.08	−0.21	6.33	−2.28
meta	9.21	−0.09	6.67	−2.38
para	9.43	0.47	7.06	−1.86

TABLE 5: Partition Functions for the OH and Methyl Internal Rotation of the Side Chain Transition State and Toluene, Calculated as Vibrations (Q_{vib}) and Hindered Internal Trotations (Q_{hind}) at 298.15 K Using BHandHLYP/6-311++G Data**

	Q_{vib}	Q_{hind}
OH	2.44	5.07
methyl (TS$_s$)	5.05	19.62
methyl (toluene)	8.75	10.69

TABLE 6: Partial Rate Coefficients (cm^3 $molecule^{-1}$ s^{-1}), Tunneling Corrections and Branching Ratio, $\Gamma = k_{ring}/k_{overall}$ (Eq 12), as a Function of Temperature

T (K)	methyl	κ	ortho	κ	meta	κ	para	κ	overall	Γ
275	1.89×10^{-13}	6.23	1.04×10^{-16}	25.00	1.10×10^{-16}	29.40	2.99×10^{-17}	33.20	1.89×10^{-13}	0.13
298.15	2.40×10^{-13}	4.46	1.65×10^{-16}	14.90	1.80×10^{-16}	17.00	5.05×10^{-17}	18.70	2.40×10^{-13}	0.16
299	2.42×10^{-13}	4.41	1.68×10^{-16}	14.70	1.83×10^{-16}	16.70	5.14×10^{-17}	18.40	2.43×10^{-13}	0.17
300	2.45×10^{-13}	4.35	1.71×10^{-16}	14.40	1.87×10^{-16}	16.40	5.26×10^{-17}	18.00	2.45×10^{-13}	0.17
311	2.72×10^{-13}	3.83	2.12×10^{-16}	11.80	2.35×10^{-16}	13.20	6.68×10^{-17}	14.40	2.73×10^{-13}	0.19
323	3.04×10^{-13}	3.38	2.67×10^{-16}	9.65	2.99×10^{-16}	10.70	8.63×10^{-17}	11.60	3.05×10^{-13}	0.21
325	3.10×10^{-13}	3.32	2.77×10^{-16}	9.36	3.11×10^{-16}	10.40	9.00×10^{-17}	11.20	3.10×10^{-13}	0.22
340	3.52×10^{-13}	2.90	3.64×10^{-16}	7.56	4.16×10^{-16}	8.29	1.23×10^{-16}	8.85	3.53×10^{-13}	0.26
350	3.82×10^{-13}	2.68	4.35×10^{-16}	6.65	5.02×10^{-16}	7.25	1.50×10^{-16}	7.70	3.83×10^{-13}	0.28
375	4.61×10^{-13}	2.26	6.66×10^{-16}	5.06	7.87×10^{-16}	5.44	2.41×10^{-16}	5.71	4.63×10^{-13}	0.37
400	5.46×10^{-13}	1.97	9.93×10^{-16}	4.04	1.20×10^{-15}	4.30	3.78×10^{-16}	4.48	5.48×10^{-13}	0.47
425	6.35×10^{-13}	1.75	1.44×10^{-15}	3.35	1.78×10^{-15}	3.53	5.74×10^{-16}	3.66	6.39×10^{-13}	0.59
450	7.30×10^{-13}	1.59	2.05×10^{-15}	2.86	2.58×10^{-15}	3.00	8.48×10^{-16}	3.09	7.36×10^{-13}	0.74
475	8.30×10^{-13}	1.46	2.84×10^{-15}	2.50	3.65×10^{-15}	2.61	1.22×10^{-15}	2.68	8.37×10^{-13}	0.92
500	9.34×10^{-13}	1.36	3.87×10^{-15}	2.23	5.05×10^{-15}	2.32	1.73×10^{-15}	2.37	9.45×10^{-13}	1.13
525	1.04×10^{-12}	1.28	5.17×10^{-15}	2.02	6.86×10^{-15}	2.09	2.38×10^{-15}	2.13	1.06×10^{-12}	1.36
550	1.16×10^{-12}	1.21	6.79×10^{-15}	1.85	9.16×10^{-15}	1.91	3.23×10^{-15}	1.94	1.18×10^{-12}	1.63
575	1.28×10^{-12}	1.15	8.79×10^{-15}	1.71	1.20×10^{-14}	1.76	4.30×10^{-15}	1.79	1.31×10^{-12}	1.92
600	1.41×10^{-12}	1.10	1.12×10^{-14}	1.60	1.55×10^{-14}	1.64	5.63×10^{-15}	1.66	1.44×10^{-12}	2.25
800	2.65×10^{-12}	0.87	5.41×10^{-14}	1.11	8.11×10^{-14}	1.13	3.17×10^{-14}	1.14	2.82×10^{-12}	5.92
1000	4.33×10^{-12}	0.76	1.67×10^{-13}	0.92	2.63×10^{-13}	0.93	1.08×10^{-13}	0.94	4.87×10^{-12}	11.05

energies of the transition states and products, calculated at the BHandHLYP and CCSD(T)//BHandHLYP levels, both with the /6-311++G(d,p) basis set, are reported in Table 4. These values include the ZPE corrections. Imaginary frequencies at the transition states are also given; they lie at about 1980 cm^{-1}, indicating tighter transition states than in the case of the side chain hydrogen abstraction, which are characterized by imaginary frequencies about 1350 cm^{-1} with the same method. A slight preference for ortho hydrogen abstraction is observed with both methods. The meta position would be expected to be the least activated position, yet its energy barrier turns out to be slightly smaller than the one for a para hydrogen atom. Results are consistent with both methods employed. The CCSD(T) energy barriers are 6.3 and 6.7 kcal/mol for the ortho and meta positions, respectively. It was not possible to obtain a converged value for the para transition state reaction at the CCSD(T) level: after 150 cycles, the calculation had not converged. Because the E_a values are so close, and the para activation barrier is the smallest, its CCSD(T) value can safely be estimated to be about 7.06 kcal/mol. No stabilizing interactions are observed in the transition state structures, which explains why the three transition states have very close energy values and also very similar imaginary frequencies.

Reaction energies corrected for ZPE, are also reported in Table 4. Ortho hydrogen abstraction yields the most stable product at the BHandHLYP level, but a small inversion is observed at the CCSD(T) level, and there, the meta product is favored. Differences, however, are very small and all three products lie about 2 kcal/mol below reactants.

Reaction profiles are shown in Figure 4. In this figure, the methyl abstraction is also represented for comparison. The prereactive complex occurs only in the methyl hydrogen abstraction.

3.2. Kinetics. Four rate constant coefficients have been determined in this work. Partial and total rate equations have been obtained for the side chain and ring OH hydrogen abstraction in toluene.

As discussed in the methodology section, the calculation of rate constants involves the determination of the correct partition functions, in which internal rotations with rotational barriers smaller than 3.0 kcal/mol are treated as rotations rather than vibrations. For TS_s, barriers were determined for the internal rotation of OH and CH_3 around their axis, using the BHandHLYP/6-311++g(d,p) method. For the OH group the barrier height is found to be about 0.48 kcal/mol, whereas the one for the methyl group is 2.96 kcal/mol. Thus, these internal rotations will be taken into account to correct the side chain transition state partition function. In Table 5, the partition functions at 298 K, calculated both as vibrations and as hindered rotations, are reported for the OH internal rotation motion in TS_s and for the CH_3 group internal rotation in TS_s and in toluene. It can be seen that using the vibration instead of the internal rotation expression introduces a large error in the total vibrational partition function. The rate constant for the side chain hydrogen abstraction would be too small by a factor of about 10 (a factor of 2 for the methyl group, due to the ratio between its contribution in TS_s and toluene, and a factor of 5 for the OH group).

In the case of TS_r, only the OH internal rotation has to be analyzed, because the methyl torsion cancels in the partition function ratio in the rate constant expression. An energy scan as a function of the corresponding dihedral angle gives a barrier of more than 6 kcal/mol, and it is clear that this motion can safely be considered as a vibration.

The calculation of the rate constants was performed using eq 11 and the program TheRate, in the 275−1000 K temperature range. Results are listed in Table 6 for the toluene reaction. They include the hindered internal rotations corrections and the tunneling factor, calculated using the Eckart formula for the asymmetric barrier. The symmetry numbers in free toluene and in TS_s have been taken to be 6 and 2, respectively. Rate constants and tunneling factors are reported as a function of temperature for the side chain abstraction and for the ortho, meta and para ring abstraction. Overall rate constants are also given. The branching ratio for ring abstractions with respect to the overall ring and side chain abstractions is given in the last column as a function of temperature:

$$\Gamma = \frac{k_{ring}}{k_{overall}} \times 100 \tag{12}$$

In agreement with the results of Tully et al.,[2] at low temperature the reaction proceeds almost exclusively through side chain abstraction, whereas at 1000 K ring abstractions account for about 11% of the total reaction.

As can be observed in Table 6, the calculated tunneling coefficient in the side chain abstraction varies from 6.23 at 275

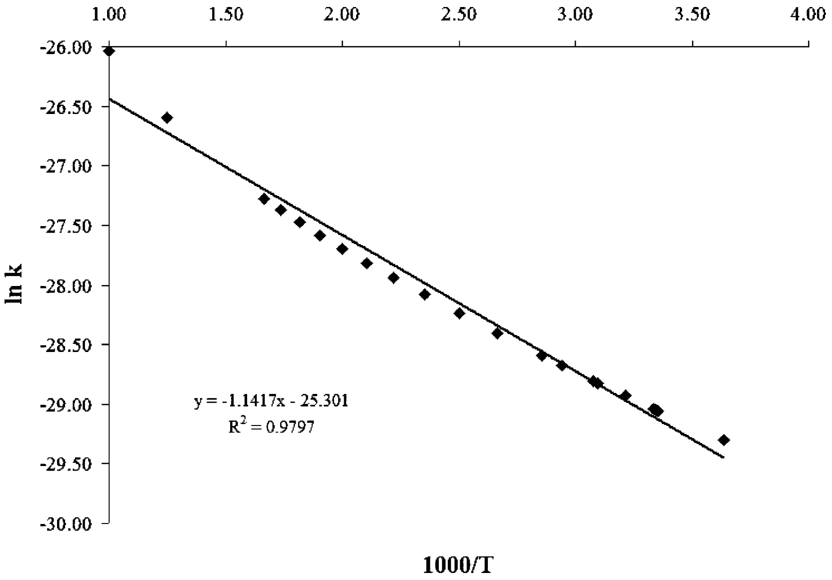

Figure 5. Behavior of ln k_{overall} as a function of 1000/T in the 275−1000 K range.

TABLE 7: Comparison between Theoretical and Experimental Rate Constant,[8] k (cm^3 molecule^{-1} s^{-1}), at Different Temperatures

	theoretical (overall)	ref 2	ref 6	ref 7
250	1.44×10^{-13}			
275	1.89×10^{-13}			
298.15	2.40×10^{-13}		4.25×10^{-13}	
299	2.43×10^{-13}		4.29×10^{-13}	
300	2.45×10^{-13}		4.33×10^{-13}	
350	3.83×10^{-13}		6.61×10^{-13}	
400	5.48×10^{-13}		9.41×10^{-13}	1.14×10^{-12}
450	7.35×10^{-13}		1.27×10^{-12}	1.45×10^{-12}
500	9.45×10^{-13}	1.55×10^{-12}	1.66×10^{-12}	1.78×10^{-12}
550	1.18×10^{-12}	1.97×10^{-12}	2.1×10^{-12}	2.12×10^{-12}
600	1.44×10^{-12}	2.4×10^{-12}	2.59×10^{-12}	2.47×10^{-12}
800	2.82×10^{-12}	4.12×10^{-12}	5.08×10^{-12}	3.96×10^{-12}
1000	4.87×10^{-12}	5.7×10^{-12}	8.43×10^{-12}	5.53×10^{-12}

K to 0.76 at 1000 K. At 298 K it is 4.46. This result may be compared with the tunneling factors at 298 K obtained by Bravo et al.[17] for OH hydrogen abstraction from primary alkanes using the same method of calculation (BHandHLYP) and the 6-311G(d,p) basis set. They report values of 30.56 for methane, 6.92 for ethane, 6.58 for primary propane, 4.93 for isobutane and 6.29 for primary *n*-butane.

The overall calculated rate constants for toluene are plotted in Figure 5 for the 275−1000 K temperature range. The influence of temperature on the overall rate coefficient within this range has been interpreted in terms of the Arrhenius equation.[37] An overall Arrhenius expression for the rate constant can be expressed as

$$k = 1.03 \times 10^{-11} e^{-2.27/RT} \tag{13}$$

In Table 7, we have compared our calculated rate constant coefficients at different temperatures with the experimental data available in the NIST Data Base.[8] At low temperatures, our calculated rate coefficients are slightly underestimated if compared with the experimental results of Knispel et al.[6] However, at high temperatures, our results are in very good agreement with the ones reported in refs 2 and 6. A discrepancy by a factor of about 2 is observed with the data of Baulch et al.[7] at 400 K, but the agreement between our data and all available experimental results becomes excellent at about 800 K.

TABLE 8: Arrhenius Parameters A (cm^3 molecule^{-1} s^{-1}) and E_a (kcal/mol) Obtained from Data in Different Temperature Ranges[a]

	E_a	A
	500−1000 K	
exptl[2]	2.58	2.09×10^{-11}
theoretical	3.24	2.31×10^{-11}
	299−1000 K	
expl[6]	2.41	2.16×10^{-11}
theoretical	2.33	1.09×10^{-11}
	400−1000 K	
exptl[7]	2.10	1.50×10^{-11}
theoretical	2.82	1.69×10^{-1}

[a] Experimental values from an Arrhenius plot using data in the NIST[8] Data Base.

We have represented the data of Tully et al.,[2] Knispel et al.[6] and Baulch et al.[7] in the form of an Arrhenius-type plot, and the corresponding Arrhenius parameters have been obtained. They are given in Table 8 for the overall reaction, and compared with the calculated results. An excellent agreement is observed, both for the preexponential factor and for the Arrhenius activation energy.

The calculated branching ratios confirm the proposal of Tully et al.[2] that, at high temperatures, abstraction of ring hydrogen atoms becomes nonnegligible. However, our results indicate a considerably smaller contribution from ring abstraction channels than estimated by Tully et al. from a simple comparison between the overall OH abstraction reaction rate constants in benzene and toluene. Although these authors suggest a 20% ring abstraction at 500 K, calculations predict that this branching ratio occurs well above 1000 K.

4. Conclusion

The employed methodology of geometry optimization and frequency calculations at the BHandHLYP/6-311++G(d,p) followed by CCSD(T) calculation with the same basis set is found to yield excellent results for the potential energy calculations along the reaction coordinate in the OH hydrogen abstraction reaction of side and ring hydrogen atoms in toluene. The use of internal rotations partition functions to replace the corresponding vibrational partition functions in the appropriate cases is essential in the calculation of the rate constant coefficients of the side chain abstraction.

Our results suggest that side chain abstraction occurs through a complex mechanism which includes the reversible formation of a reactant complex previously described; the important role of this complex in the correct calculation of the tunneling correction is underestimated if collisional stabilization is not assumed. The very good agreement between calculated and experimentally determined rate coefficients supports the proposed mechanism.

Ring abstraction is nonnegligible at high temperatures but remains relatively small, being about 11% at 1000 K.

An excellent agreement between theoretical and experimental results is obtained for the overall rate constant coefficient of the OH hydrogen abstraction from toluene.

Acknowledgment. We gratefully acknowledge the financial support from the SEP-CONACYT Project SEP-2004-C01-46167, from PROMEP through a grant to establish the "Quantum Chemistry and Molecular Simulation" network, and from grant DGAPA UNAM (PAPIIT-IN203206-2), Mexico.

Supporting Information Available: Tables of the electronic energies, ZPE corrections and Cartesian coordinates geometries for all channels of the toluene + OH abstraction reaction. This material is available free of charge via the Internet at http://pubs.acs.org.

References and Notes

(1) Finlayson-Pitts, B. J.; Pitts, J. N. *Atmospheric Chemistry: Fundamentals and Experimental Techniques*; Wiley-Interscience: New York, 1986.

(2) Tully, F. P.; Ravishankara, A. R.; Thompson, R. L.; Nicovich, J. M.; Shah, R. C.; Kreutter, N. M.; Wine, P. H. *J. Phys. Chem.* **1981**, *81*, 2262.

(3) Atkinson, R. *J. Phys. Chem. Ref. Data, Monograph 1* **1989**, 1.

(4) Atkinson, R. *J. Phys. Chem. Ref. Data, Monograph 2* **1994**, 1.

(5) Perry, R. A.; Atkinson, R.; Pitts, J. N., Jr. *J. Phys. Chem.* **1977**, *81*, 296.

(6) Knispel, R.; Koch, R.; Siese, M.; Zetzsch, C. *Ber. Bunsen-Ges. Phys. Chem.* **1990**, *94*, 1375.

(7) Baulch, D. L.; Cobos, C. J.; Cox, R. A.; Esser, C.; Frank, P.; Just, Th.; Kerr, J. A.; Pilling, M. J.; Troe, J.; Walker, R. W.; Warnatz, J. *J. Phys. Chem. Ref. Data* **1992**, *21*, 411.

(8) The NIST Chemical Kinetics Database, NIST Standard Reference Database; US Department of Commerce, Technology Administration, National Institute of Standards and Technology, Gaithersburg, MD, 17-2Q98.

(9) Markert, F.; Pagsberg, P. *Chem. Phys. Lett.* **1993**, *209*, 445.

(10) Andino, J. M.; Smith, J. N.; Flagan, R. C.; Goddard, W. A., III; Seinfeld, J. H. *J. Phys. Chem.* **1996**, *100*, 10967.

(11) Uc, V. H.; García-Cruz, I.; Hernández-Laguna, A.; Vivier-Bunge, A. *J. Phys. Chem. A* **2000**, *104*, 7847.

(12) Bartolotti, L. J., Edney, E. O. *Chem. Phys. Lett.* **1995** *245*, 119.

(13) Suh, I.; Zhang, D.; Zhang, R.; Molina, L. T.; Molina, M. J. *Chem. Phys. Lett.* **2002**, *364*, 454.

(14) Tokmakov, I. V.; Lin, M. C. *J. Chem. Phys. A* **2002**, *106*, 11309.

(15) García-Cruz, I.; Uc, V. H.; Vivier-Bunge, A.; Smeyers, Y. G. *Proceedings of the III UNAM-Cray Supercomputing Conference, in Computational Chemistry and Chemical Engineering*; Cisneros G., Cogordan, J. A., Castro, M., Wang, C., Eds.; World Scientific: Singapore, 1997; p 168.

(16) García-Cruz, I.; Ruíz-Santoyo, M. E.; Alvarez-Idaboy J. R.; Vivier-Bunge, A. *J. Comput. Chem.* **1999**, *20* 845.

(17) Bravo-Pérez, G.; Alvarez-Idaboy, J. R.; Galano Jiménez A.; Cruz-Torres, A., *Chem. Phys.* **2005**, *310*, 213.

(18) Frisch, M. J.; Trucks, G. W.; Schlegel, H. B.; Scuseria, B. G., Robb, M. A.; Cheeseman, J. R.; Zakrzewski, V. G.; Montgomery, J. A.; Stratmann, R. E.; Burant, J. C.; Dapprich, S.; Millam, J. M.; Daniels, A. D.; Kudin, K. N.; Strain, M. C.; Karkas, O.; Tomasi, J.; Barone, V.; Cossi, M.; Cammi, R.; Mennucci, B.; Pomelli, C.; Adamo, C.; Clifford, S.; Ochterski, G.; Petersson, G. A., Ayala, P. Y., Cui, Q.; Morokuma, K.; Malick, D. K.; Rabuck, A. D.; Raghavachari, K.; Foresman, J. B.; Cioslowski, J.; Ortiz, J. V.; Stefanov, B. B.; Liu, G.; Liashenko, A.; Piskorz, P.; Komaromi, I.; Gomperts, R.; Martin, R. L.; Fox, D. J.; Keith, T. A.; Al-Laham, M. A.; Peng, C. Y.; Nanayakkara, A.; Gonzalez, V.; Challacombe, M.; Gill, P. M. W.; Johnson, B. G.; Chen, W.; Wong, M. W.; Andres, J. L.; Head-Gordon, M.; Replogle, E. S.; Pople, J. A. *Gaussian98*, revision A.7; Gaussian, Inc.: Pittsburgh, PA, 1998.

(19) Uc, V. H.; García-Cruz, I.; Grand, A.; Vivier-Bunge, A. *J. Phys. Chem. A* **2001**, *105*, 6226.

(20) Uc, V. H.; Grand, A.; Hernández-Laguna, A.; Vivier-Bunge, A. *Phys. Chem. Chem. Phys.* **2002**, *4*, 5730.

(21) Becke, A. D. *J. Chem. Phys.* **1993** *98*, 5648.

(22) González, C.; Schlegel, H. B. *J. Phys. Chem.* **1990**, *94*, 5523.

(23) Singleton D. L.; Cvetanovic, R. J. *J. Am. Chem. Soc.* **1976**, *98*, 6812.

(24) Pilling, M. J.; Seakins, P. W. *Reaction Kinetics*; Oxford University Press: New York, 1996.

(25) Truong, T. N.; Duncan, W. T. TheRate 1.0. University of Utah, 1993.

(26) Eckart, C. *Phys. Rev.* **1930**, *35*, 1303.

(27) Galano, A.; Alvarez-Idaboy, J. R.; Vivier-Bunge, A. *J. Chem. Educ.* **2006**, *83*, 481.

(28) Ayala, P. Y.; Schlegel, H. B. *J. Chem. Phys.* **1998**, *108*, 2314.

(29) Sosa, C.; Schlegel, H. B. *J. Am. Chem. Soc.* **1987**, *109*, 4193.

(30) Díaz-Acosta, I.; Alvarez-Idaboy J. R.; Vivier-Bunge, A. *Int. J. Chem. Kinet.* **1999**, *31*, 29.

(31) Alvarez-Idaboy, J. R.; Mora-Diez, N.; Boyd, R. J.; Vivier-Bunge, A. *J. Am. Chem. Soc.* **2001**, *123*, 2018.

(32) Galano, A.; Alvarez-Idaboy, J. R.; Ruíz-Santoyo, M. E.; Vivier-Bunge, A. *J. Phys. Chem. A.* **2002**, *106* 9520.

(33) Sekuŝak, S.; Sabljic, A. *Chem. Phys. Lett.* **1997**, *272*, 353.

(34) Smith, I. W. M.; Ravishankara, A. R. *J. Phys. Chem. A* **2002**, *106*, 4798.

(35) Bader, R. F. W. *Atoms in Molecules*; Clarendon Press: Oxford, U.K., 1990.

(36) Bader, R. F. W. *Chem. Rev.* **1991**, *91*, 893.

(37) Arrhenius, S. *Z. Phys. Chem.* **1889**, *4*, 226.